Available online at www.sciencedirect.com

SCIENCE DIRECT®

Inorganica Chimica Acta 358 (2005) 4489–4496

Inorganica Chimica Acta

www.elsevier.com/locate/ica

Oxo-rhenium(V) complexes with analogs of bis(diphenylphosphino)ethane

Olivier Sigouin, André L. Beauchamp *

Département de chimie, Université de Montréal, C.P. 6128 Succ. Centre-ville, Montréal, QC, Canada H3C 3J7

Received 8 April 2005; received in revised form 30 July 2005; accepted 30 July 2005
Available online 21 September 2005

Abstract

Compounds of the types $ReOCl_3(L–L)$ and $ReOCl_2(OEt)(L–L)$ with bis(diphenylphosphino)ethene (dppen) and bis(diphenylphosphino)ferrocene (dppf) were prepared by reacting the diphosphine with $ReOCl_3(OPPh_3)(Me_2S)$. The $ReOCl_3(L–L)$ compound with bis(diphenylarsino)ethane (dpae) was prepared similarly. Crystallographic work on $ReOCl_3$(dppen) and $ReOCl_3$(dpae) confirmed the approximate octahedral environment of the metal and the presence of a Cl ligand *trans* to the Re=O bond. The $ReOCl_2(OEt)(L–L)$ compounds contain a *trans*O=Re-OEt unit. The visible spectra of both types of compounds include a two-component d–d absorption pattern originating from the spin-allowed excitation of a d electron from the interaxial d orbital in the equatorial plane to the empty d_{xz} and d_{yz} orbitals. For $ReOCl_2(OEt)$(dppf), these bands are masked by strong transitions taking place in the ferrocene moiety. The absorptions of the other systems are not greatly displaced compared to the similar dppe compounds, a small decrease in the transition energy being noted for the dpae complex.

Keywords: Rhenium; Diphosphine; Diarsine; Crystal structure; d–d Electron transitions

1. Introduction

Compounds giving rise to electronic transitions between low-spin and high-spin states at low energy cost present considerable interest, since they may provide a basis to develop molecular switches and devices for efficient information storage. The d^2 oxo-rhenium(V) core is a stable unit in which the ground state is low-spin and diamagnetic, since the strong π bonds formed via the oxygen p_x and p_y orbitals raise the d_{xz} and d_{yz} orbitals (LUMO) above the other interaxial d orbital (HOMO), in which the two d electrons are paired. However, if the HOMO–LUMO gap could be reduced and become comparable with the pairing energy, the molecule could adopt a high-spin triplet ground state or possess a readily accessible high-spin excited state that could be involved in spin-crossover processes.

Following the initial study which revealed that the HOMO–LUMO gap is relatively small in $ReOCl(P \sim O)_2$ compounds containing bidentate mixed $P \sim O^-$ ligands [1], various series of related compounds were considered in order to gain insight in the factors affecting the HOMO–LUMO gap in these system. We examined $ReOX_3$(dppe) and $ReOX_2(OR)$(dppe) compounds, where the coordination sphere remained close to that of the $ReOCl(P \sim O)_2$ species and the equatorial *cis*-P,P arrangement was provided by bis(diphenylphosphino)ethane (dppe) [2]. The presence of a strong π-donor RO^- group *trans* to the Re=O bond in $ReOX_2(OR)$(dppe) was found to produce an energy gap greater than those of the $ReOX_3$(dppe) compounds, where the *trans* position is occupied by a halogen. In the present study, we are looking at related compounds in which the central $–CH_2–CH_2–$ link of dppe is replaced by the more rigid –CH=CH– unit or the relatively large ferrocene unit. An analogous complex with bis(diphenylarsino)ethane (dpae) is also included. The paper reports the preparation, characterization and

---

* Corresponding author. Tel.: +1 514 343 6446; fax: +1 514 343 7586.
E-mail address: andre.beauchamp@umontreal.ca (A.L. Beauchamp).

0020-1693/$ - see front matter © 2005 Elsevier B.V. All rights reserved.
doi:10.1016/j.ica.2005.07.038

UV–visible spectra of these complexes, together with crystallographic work on $ReOCl_3$(dppen) and $ReOCl_3$(dpae). Although substitution of the central unit in the ligand affects the bite of the ligands and the extent of communication between the two donor atoms, no drastic changes were detected in the HOMO–LUMO gap.

2. Experimental

2.1. Reactants and methods

$KReO_4$, the diphosphines, the diarsine and all other reactants were obtained from Aldrich and used without further purification. $ReOCl_3(OPPh_3)(Me_2S)$ was prepared from $ReOCl_3(PPh_3)_2$ [3] as described in the literature [4,5]. Deuterated solvents were purchased from Aldrich.

IR spectra were recorded on Perkin–Elmer Spectrum One (4000–400 cm^{-1}, KBr pellets) or Bio-Rad Excalibur FTS 3000FX (4000–200 cm^{-1}, CsI pellets) spectrometers. The NMR spectra were measured with Bruker AV-300, AMX-300, AV-400 or ARX-400 spectrometers. For the ^1H spectra, the residual solvent signal (DMSO-d_6, 2.50 ppm; acetone-d_6, 2.17 ppm; $CDCl_3$, 7.26 ppm) was used as internal reference. H_3PO_4 was used as an external reference ($\delta = 0$) for the $^{31}P\{^1H\}$ spectra. Electronic spectra of chloroform solutions were recorded in quartz cells with a UV–Vis-NIR Cary 5E spectrometer. Elemental analyses were run at the Laboratoire d'Analyse Élémentaire de l'Université de Montréal.

2.2. Preparation of the $ReOCl_3$(L–L) compounds

All compounds were prepared from $ReOCl_3(OPPh_3)(Me_2S)$. In a typical run, this precursor (1.56 mmol) was added to a refluxing solution of the diphosphine (1.63 mmol) in THF (25 mL). A blue suspension formed immediately and after stirring for 90 min, a blue solid was collected by filtration, washed with ethanol and diethyl ether, and dried in vacuo. Details for each compound are provided below.

2.2.1. $ReOCl_3$(dppe)

Reaction time: 90 min. Blue solid, yield: 84%. *Anal.* Calc. for $C_{26}H_{24}Cl_3OP_2Re$: C, 44.17; H, 3.42. Found: C, 44.10; H 3.33%. ^1H NMR, $^{31}P\{^1H\}$ NMR and IR data correspond to those reported earlier [2].

2.2.2. $ReOCl_3$(dppen)

Reaction time: 3 h. In this case, the product was soluble. The mixture was evaporated to dryness and upon addition of CH_2Cl_2, a blue solid was obtained from a green solution. Yield: 44%. *Anal.* Calc. for $C_{26}H_{22}Cl_3OP_2Re$: C, 44.30; H, 3.15. Found: C, 44.13; H, 2.48%. ^1H NMR (DMSO-d_6) (ppm) δ: 8.88 (m, 2H, $H_{C=C}$, second-order signal, see next section), 7.94 (m, 4H, H_o), 7.86 (m, 4H, H_o), 7.51 (m, 12H, $H_{m,p}$). $^{31}P\{^1H\}$ NMR (DMSO-d_6) (ppm) δ : 20.69 (s). IR (CsI, cm^{-1}): 989 (s) ν(Re=O); 320 (w), 278 (w) ν(Re–Cl).

2.2.3. $ReOCl_3$(dppf)

Reaction time: 9 days. Green solid, yield: 41%. The solid retains 0.4 mol of diethyl ether. *Anal.* Calc. for $C_{35.6}H_{32}Cl_3FeO_{1.4}P_2Re$: C, 47.90; H, 3.61. Found: C, 47.99; H, 3.41%. ^1H NMR (acetone-d_6) (ppm) δ: 7.98 (m, 4H, H_o), 7.77 (m, 4H, H_o), 7.40–7.56 (m, 12H, $H_{m,p}$), 5.37 (m, 2H, $H_{ferrocene}$), 4.94 (m, 2H, $H_{ferrocene}$), 4.68 (m, 2H, $H_{ferrocene}$), 4.52 (m, 2H, $H_{ferrocene}$). $^{31}P\{^1H\}$ NMR (acetone-d_6) (ppm) δ: −25.90 (s). Similar NMR data were obtained in $CDCl_3$ [6] or CD_2Cl_2 [7]. IR (CsI, cm^{-1}): 966 (s) ν(Re=O); 326 (w), 278 (w) ν(Re–Cl).

2.2.4. $ReOCl_3$(dpae)

Reaction time: 20 h. Blue–green solid, yield: 91%. *Anal.* Calc. for $C_{26}H_{24}As_2Cl_3ORe$: C, 39.29; H, 3.04. Found: C, 39.33; H, 3.12%. ^1H NMR (DMSO-d_6) (ppm) δ: 7.93 (m, 4H, H_o), 7.77 (m, 4H, H_o), 7.47–7.53 (m, 12H, $H_{m,p}$), 3.40 (m, 2H, CH_2, partly masked by water peak), 2.95 (m, 2H, CH_2). IR (CsI, cm^{-1}): 980 (s) ν(Re=O); 320 (w), 278 (w) ν(Re–Cl).

2.3. Preparation of the $ReOCl_2$(OEt)(L–L) compounds

These compounds were obtained by the same method as above, but ethanol was used as the solvent. In a typical run, $ReOCl_3(OPPh_3)(Me_2S)$ (0.16 mmol) was stirred in a refluxing solution of dppe (0.16 mmol) in ethanol (10 mL). The initially green suspension turned purple slowly. After 6 days, a purple solid was collected by filtration, washed with ethanol and diethyl ether, and dried in vacuo.

2.3.1. $ReOCl_2$(OEt)(dppe)

Purple solid, yield: 64%. *Anal.* Calc. for $C_{28}H_{29}Cl_2O_2P_2Re$: C, 46.93; H, 4.08. Found: C, 46.66; H, 3.94%. ^1H NMR, $^{31}P\{^1H\}$ NMR (DMSO-d_6) and IR (CsI, cm^{-1}) data as reported earlier [2].

2.3.2. $ReOCl_2$(OEt)(dppen)

Reaction time: 9 days. Purple solid, yield: 69%. *Anal.* Calc. for $C_{28}H_{27}Cl_2O_2P_2Re$: C, 47.06; H, 3.81. Found: C, 46.68; H, 3.66%. ^1H NMR ($CDCl_3$) (ppm) δ: 8.09 (m, 4H, H_o), 7.97 (m, 2H, $H_{C=C,}$ second-order signal, see next section), 7.80 (m, 4H, H_o), 7.43 (m, 12H, $H_{m,p}$), 2.08 (q, 2H, $J = 7.0$ Hz, OCH_2CH_3), −0.09 (t, 3H, $J = 7.0$ Hz, OCH_2CH_3). $^{31}P\{^1H\}$ NMR ($CDCl_3$) (ppm) δ: 31.50 (s). IR (CsI, cm^{-1}): 944 (s) ν(Re=O); 282 (w) ν(Re–Cl).

2.3.3. $ReOCl_2$(OEt)(dppf)

Reaction time: 7 days. Yellow, solid, yield: 41%. *Anal.* Calc. for $C_{36}H_{33}Cl_2FeO_2P_2Re$: C, 49.55; H, 3.81. Found: C, 49.37; H, 3.82%. ^1H NMR (acetone-d_6) (ppm) δ: 7.99 (m, 4H, H_o), 7.89 (m, 4H, H_o), 7.44–7.55 (m, 12H, $H_{m,p}$), 4.84 (m, 2H, $H_{ferrocene}$), 4.80 (m, 2H, $H_{ferrocene}$), 4.61 (m, 2H, $H_{ferrocene}$), 4.48 (m, 2H, $H_{ferrocene}$), 2.94 (q, 2H, $J = 7.0$ Hz, OCH_2CH_3), 0.34 (t, 3H, $J = 7.0$ Hz, OCH_2CH_3). $^{31}P\{^1H\}$ NMR (acetone-d_6) (ppm) δ: −9.13 (s). IR (CsI, cm^{-1}): 951 (s) ν(Re=O); 275 (w) ν(Re–Cl).

2.4. Crystallographic measurements and structure determination

Dark-blue plates of $ReOCl_3$(dppen) were obtained by slow diffusion of $CHCl_3$ into a CH_2Cl_2 solution. The crystallographic study was carried out with an Enraf-Nonius CAD-4 diffractometer (Cu Kα radiation) controlled by the CAD-4 software [8]. The reduced cell was initially determined from 20 to 25 spots located on a preliminary rotation photograph and centered in the detector aperture. Accurate cell parameters were then calculated from the positions of 25 high-angle reflections centered with the SETANG and DETTH procedures. The intensities were recorded by $\omega/2\theta$ scan. Possible crystal decomposition was monitored by measuring five standard reflections every hour. Space group $P2_1/n$ was defined unambiguously from the monoclinic Laue symmetry and systematic absences ($h0l$, $h+l \neq 2n$ and $0k0$, $k \neq 2n$). All data in the whole sphere were collected at room temperature. An absorption correction based on crystal geometry was applied. The data were finally corrected for the effects of Lorentz and polarization, and averaged to provide the basic two-octant set.

The Re atom was located by the heavy-atom method and the remaining non-hydrogen atoms were located by the standard Fourier technique. The SHELXTL system [9] was used for all calculations. The structure was refined on F_o^2 using all reflections. The H atoms were fixed using a riding model with $U_{iso} = 1.2 \times U_{eq}$ of the atom to which they are bonded. The crystal data are listed in Table 1.

Blue–green crystals of $ReOCl_3$(dpae) were obtained by slow diffusion of $CHCl_3$ into a CH_2Cl_2 solution. A crystal was mounted on a Bruker SMART CCD 2K diffractometer (Cu Kα radiation) controlled by the SMART software [10]. Sets of 30 oscillation frames of 0.3° over a range of 9° were recorded in four regions of the reciprocal space, from which the reduced cell was determined by least-squares refinement. For data collection, frames were recorded for different orientations of the crystal and detector so as to cover at least 95% of the reciprocal sphere. At the end, the first 101 frames were remeasured and the intensities of the 907 reflections did not show any decomposition of the crystal. The frames were analyzed with the SAINT software [11], which determined the intensity and the position of each spot. Accurate cell parameters were obtained by least-squares refinement over the positions of the whole data set. An absorption correction based on crystal geometry was applied.

Structure resolution required considerable effort because both pseudo-symmetry and disorder are present. Space group $P2_1/c$ was considered first on the basis of the monoclinic Laue symmetry and systematic absences ($h0l$, $l \neq 2n$ and $0k0$, $k \neq 2\,n$), although uncertainty remained concerning the $0k0$ k odd condition, a few of these reflections showing intensity somewhat above background. A reasonable solution was obtained in $P2_1/c$, but all phenyl rings showed disorder or very large thermal ellipsoids. The R factor could not be reduced below 0.12. Resolution was then attempted in the $P2/c$ and Pc groups, assuming that only the $h0l$ $l \neq 2n$ condition was strictly obeyed. No solution emerged in $P2/c$, but a reasonable model was obtained in Pc. This model was in fact a superstructure of the $P2_1/c$ solution, in which the two molecules related by the $P2_1/c$ inversion center have become symmetry independent. Refinement proceeded slowly, but normally, in space group Pc. Peaks for C and Cl atoms of two independent $CHCl_3$ solvent molecules were found in the ΔF map and these positions were refined isotropically. Anisotropic refinement of the remaining non-hydrogen atoms, with the hydrogens constrained as above, converged to $R = 0.052$. The crystal data are listed in Table 1.

Table 1
Crystal data

	$ReOCl_3$(dpae) · $CHCl_3$	$ReOCl_3$(dppen)
Formula	$C_{27}H_{25}As_2Cl_6ORe$	$C_{26}H_{22}Cl_3OP_2Re$
Formula weight	914.25	704.94
Crystal shape	blue–green block	blue block
T (K)	223(2)	293(2)
Diffractometer	Bruker Smart CCD 2K	CAD4
Crystal system	monoclinic	monoclinic
Space group	Pc (no. 7)	$P2_1/n$ (no. 14)
a (Å)	11.4708(1)	10.184(5)
b (Å)	21.6188(1)	15.606(5)
c (Å)	13.6442(1)	16.202(5)
α (°)	90	90
β (°)	108.18(1)	95.15(3)
γ (°)	90	90
Volume (Å^3)	3214.63(4)	2565(2)
Z	4	4
d_{calc} (g/cm^3)	1.889	1.826
Reflections cell parameters	30445	25
Crystal dimensions (mm)	$0.38 \times 0.21 \times 0.09$	$0.32 \times 0.20 \times 0.12$
Radiation Cu Kα, λ (Å)	1.54178	1.54178
μ (cm^{-1})	14.43	13.42
Reflections measured	38948	36063
Reflections independent	10453 ($R_{int} = 0.049$)	4866 ($R_{int} = 0.042$)
Reflections observed ($I > 2\sigma$)	9566	3592
$R(I > 2\sigma)$[a]	0.0518	0.0344
$wR_2(I > 2\sigma)$[a]	0.1237	0.0860
$S(I > 2\sigma)$[a]	1.042	0.887

[a] $R = \sum \| F_o \| - \| F_c \| / \sum \| F_o \|$, $wR_2 = \{\sum[w(F_o^2 - F_c^2)^2] / \sum w(F_o^2)^2\}^{1/2}$, $S = \{\sum[w(F_o^2 - F_c^2)^2]/(N_{obs} - N_{param})\}^{1/2}$.

Relatively large thermal ellipsoids in phenyl rings suggest that a general disorder could exist in the structure and there is indeed evidence that the *trans* Cl–Re=O segment is involved in a subtle disorder. For molecule 2, the abnormally long Re(2)=O(2) bond (1.890(13) Å) and short Re(2)–Cl(4) bond (2.196(6) Å) indicate that these two bonds a randomly interchanged over the crystal, as reported earlier for related compounds [2,12,13]. Attempts to describe the O(2) and Cl(4) sites as a combination of non-coincident fractional O and Cl atoms did not result in any significant improvement of the crystallographic result. A similar effect is noted for molecule 1, although the bond lengths indicate that the extent of disorder is not as large. In a search for missed symmetry, the PLATON software [14] detected a certain similarity, but very significant differences between the two independent molecules.

3. Results and discussion

In previous reports, $ReOCl_3(PPh_3)_2$ or $ReOCl_3(AsPh_3)_2$ were used as starting materials to prepare the $ReOCl_3$(L–L) compounds [2,3,6,7,15]. In the present cases, the reactions (Scheme 1) were carried out in THF starting from *mer*, *trans*-O,O-$ReOCl_3(OPPh_3)(Me_2S)$ (**I**), which reduced reaction time and made purification easier. To obtain the ethoxo compounds, the reaction was run in ethanol instead of THF. Despite the fact that positions the two labile groups are *cis* to one another in the precursor (**I**), rearrangement occurred and the *fac*-trichloro (**II**) and *trans*-oxo-ethoxo products (**III**) were isolated.

3.1. IR and NMR spectroscopies

The IR spectra of the trichloro complexes show the strong IR ν(Re=O) band at 966–989 cm^{-1} expected for mono-oxo systems [16]. Two ν(Re–Cl) bands are observed at 278–280 and 320–326 cm^{-1} [13]. For the oxo-ethoxo complexes, the ν(Re=O) band appears in the 944–951 cm^{-1} range and a single ν(Re–Cl) vibration is found between 275 and 285 cm^{-1}.

A singlet in the $^{31}P\{^1H\}$ NMR spectra of the trichloro compounds is clear evidence for bidentate coordination of the diphosphine and for the *fac*-trichloro arrangement (**II**) observed in the crystal structures of the compounds with dppe [2], dppf [15] and dppen (see below). The ethoxo complexes (**III**) also give a $^{31}P\{^1H\}$ NMR singlet, in agreement with the Cl ligand *trans* to the Re=O bond being displaced, as observed for dppe complexes with various alkoxo groups [2,17]. The singlets are downfield from those of the corresponding trichloro complexes.

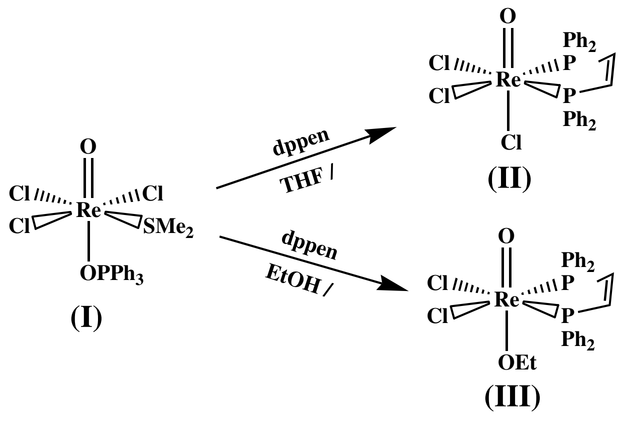

Scheme 1.

Fast inversion of the puckered chelate ring across the equatorial plane (perpendicular to Re=O) of the dppe or dpae complexes renders the two methylene groups equivalent on the NMR time scale. Since both sides of the equatorial plane are non-equivalent, two ^1H multiplets are observed between 2.9 and 3.8 ppm. For the same reason, the ferrocenyl protons of the dppf complexes show four signals between 4.48 and 5.37 ppm. Because of the anisotropic effect of the Re=O bond, the protons on the oxo side are believed to be the most deshielded [18,19]. The presence of an alkoxo group brings the multiplets closer together. The Δδ value of 0.55 ppm of $ReOCl_3$(dppe) decreases to 0.17 for the $ReOCl_2$(OEt)(dppe) [2]. For the $ReOCl_3$(dppf) and $ReOCl_2$(OEt)(dppf) pair, a similar reduction of Δδ from ~0.55 to ~0.27 ppm is noted.

For the dppen complexes, the protons are part of an AA′XX′ system and they generate the second-order pattern shown in Fig. 1. Simulation [20] was used to fit the spectra and a perfect fit was obtained for both $ReOCl_3$(dppen) and $ReOCl_2$(OEt)(dppen) with the coupling constants listed in Table 2.

The phenyl rings above the equatorial plane are not equivalent with those below and they should lead to two sets of ^1H signals. This is not detected in the spectra of the dppe complexes, where only two complicated multiplets appear in a 2:3 intensity ratio and are assigned to the *ortho* and to the *meta*/*para* protons, respectively [2]. However, for the other ligands, although the *meta*/*para* protons re-

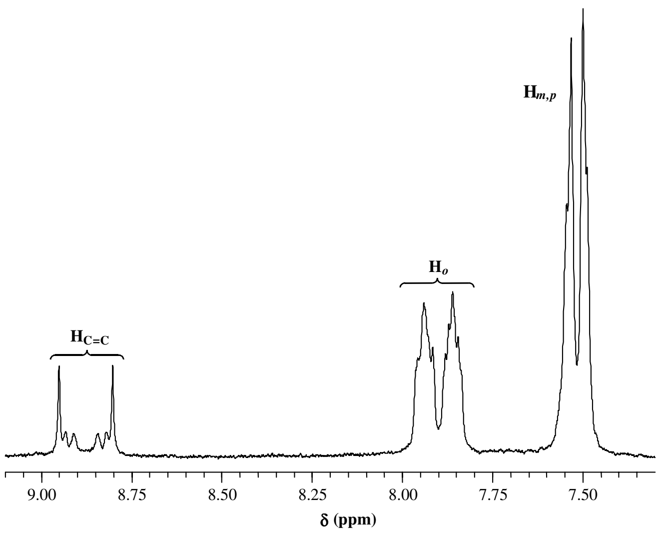

Fig. 1. Low-field ^1H NMR spectral region of $ReOCl_3$(dppen) in DMSO-d_6. The complex second-order signal at ~8.9 ppm is due to the –C(H)=C(H)– protons.

Table 2
Coupling constants (Hz) for the –C(H)=C(H)– protons in $ReOCl_3$(dppen)

$^3J_{HH'}$	9.3
$^2J_{HP}$	51.5
$^3J_{HP'}$	7.8
$^3J_{PP'}$	7.5

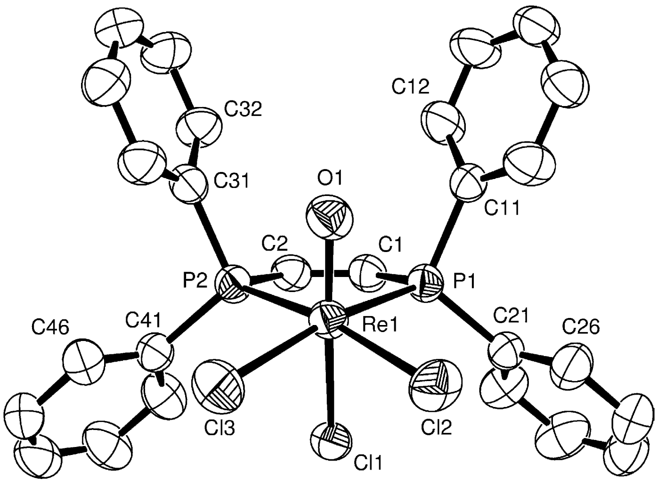

Fig. 2. ORTEP drawing of the $ReOCl_3$(dppen) molecule. Ellipsoids correspond to 30% probability. Hydrogens are omitted for simplicity. In the phenyl ring numbering scheme, the last digit corresponds to the position around the ring, starting with 1 for the *ipso* position.

main unresolved, the eight *ortho* protons split into two signals with the same intensity.

3.2. X-ray diffraction studies

In $ReOCl_3$(dppen) (Fig. 2) and $ReOCl_3$(dpae) (Fig. 3), the rhenium atom has a slightly distorted octahedral coordination. The equatorial plane consists of the P (or As) atoms of the bidentate ligand and two *cis* Cl atoms. A third Cl ligand lies *trans* to the Re=O bond. The largest deviation from octahedral coordination is the displacement of the Re from the $P(As)_2Cl_2$ plane by 0.15–0.25 Å on the oxo side, which is typical of this type of compounds. Selected distances and angles are listed in Table 3.

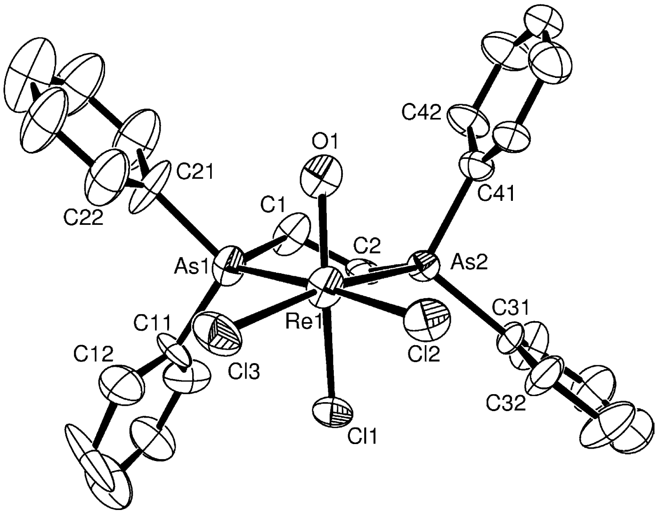

Fig. 3. ORTEP drawing of one of the two independent $ReOCl_3$(dpae) molecules. The structure of the second molecule in the asymmetric unit is very similar. Ellipsoids correspond to 30% probability. Hydrogens are omitted for simplicity. In the phenyl ring numbering scheme, the last digit corresponds to the position around the ring, starting with 1 for the *ipso* position.

3.2.1. $ReOCl_3$(dppen)

The structure of $ReOCl_3$(dppen) is actually very close to that of $ReOCl_3$(dppe) [21]. As expected, replacing the –CH_2–CH_2– connecting segment by –C(H)=C(H)– reduces the central C–C distance from 1.537 to 1.327 Å, but the P(1)–Re–P(2) bite angle is not appreciably affected (82.0° vs. 83.3° for dppe) [21]. The bond lengths in the O=Re–Cl unit remain close to those of the dppe compound. Significant differences in the Re–Cl_{eq} distances (and various other distortions) ascribed to ring puckering in the dppe compounds [2] are no longer observed here, the Re–Cl_{eq} distances being 2.385 Å. The P–C=C–P atoms are coplanar within experimental error, but the chelate ring is not planar, since the Re atom lies 0.359 Å away from this plane. The torsion angles in Table 3 show that replacing the puckered chelate ring of $ReOCl_3$(dppe) by the relatively flat ring in $ReOCl_3$(dppen) results in a considerable modification of the van der Waals envelope of the complex, not only because the P–Ph bonds are differently positioned, but also because the phenyl rings adopt different orientations. This is particularly clear for ring #1, where the Re–P–C_{ipso}–C_{ortho} torsion angles differ by 44°.

3.2.2. $ReOCl_3$(dpae)

The unit cell of $ReOCl_3$(dpae) contains two symmetry independent molecules, which are actually very similar to one another and to $ReOCl_3$(dppe) [21] (Table 3). The conformations of the puckered chelate rings are actually very close, as evidenced from the As(P)–C_{centr}–C_{centr}–As(P) and C_{centr}–C_{centr}–As(P)–C_{ortho} torsion angles. On the other hand, the Re–P–C_{ipso}–C_{ortho} angles show that the phenyl rings are oriented differently. Interestingly, for the two $ReOCl_3$(dpae) molecules, three of the phenyl rings adopt similarly orientations, whereas the remaining rings (type #2) are 90° apart.

In the equatorial plane, the Re–Cl_{eq} bond lengths (2.358–2.387 Å) agree well with the expected values, whereas the Re–As distances (2.526–2.542 Å) are normal, considering that As has a covalent radius ~0.12 Å greater than P. Clearly, there is an anomaly in the Re=O and Re–Cl_{trans} bond lengths, which differ considerably from those of the dppe complex and show large discrepancies between the two symmetry-independent molecules. This is an artifact resulting from a subtle crystallographic disorder affecting, to a different extent, both $ReOCl_3$(dpae) molecules: for some of the molecules, the O=Re–Cl_{trans} segment adopts the opposite direction in a random manner, without affecting appreciably the remaining atoms in the molecule. This problem is sometimes encountered when a complex has its van der Waals envelope largely defined by one or a few very bulky ligands, allowing small ligands (like Cl or O here) to exchange positions without disturbing the molecular structure and crystal packing [2,12,13]. Since the weighted average position is obtained from the X-ray data, the shorter bond appears longer than normal, whereas the long bond seems to be too short. Originally, these erratic bond lengths were mistakenly attributed to

Table 3
Distances (Å) and angles (°) in $ReOCl_3$(dppen) and $ReOCl_3$(dpae) · $CHCl_3$

	$ReOCl_3$(dppen) $E = P$	$ReOCl_3$(dppe) $E = P$ [21]	$ReOCl_3$(dpae) · $CHCl_3$ $E = As$	
Re=O(1)	1.669(4)	1.680	1.812(10)	1.890(13)
Re–E(1)	2.437(2)	2.429	2.539(2)	2.530(2)
Re–E(2)	2.425(2)	2.463	2.526(2)	2.542(2)
Re–Cl(1)	2.419(2)	2.445	2.355(3)	2.196(6)
Re–Cl(2)	2.384(2)	2.377	2.387(4)	2.358(4)
Re–Cl(3)	2.385(2)	2.380	2.367(4)	2.387(4)
C(1)–C(2)	1.327(8)	1.537	1.48(2)	1.51(2)
O(1)=Re–Cl(1)	164.1(2)	163.0	162.9(3)	163.4(4)
E(1)–Re–Cl(2)	167.31(6)	173.2	175.9(1)	175.9(1)
E(2)–Re–Cl(3)	168.39(6)	164.5	169.1(1)	169.0(1)
O(1)=Re–Cl(2)	100.9(2)	101.4	96.5(3)	99.1(4)
O(1)=Re–Cl(3)	102.9(2)	103.9	100.0(3)	99.6(4)
O(1)=Re–E(1)	89.2(2)	84.3	87.5(3)	84.6(4)
O(1)=Re–E(2)	90.4(2)	91.4	90.0(3)	90.2(4)
Cl(1)–Re–Cl(2)	89.51(6)	91.5	95.60(13)	93.1(2)
Cl(1)–Re–Cl(3)	89.53(7)	87.7	92.69(13)	92.0(2)
Cl(1)–Re–E(1)	77.93(6)	82.2	80.37(10)	82.91(19)
Cl(1)–Re–E(2)	78.88(6)	76.8	76.69(9)	77.47(18)
E(1)–Re–E(2)	82.01(6)	83.3	82.85(5)	82.83(6)
Cl(3)–Re–E(1)	95.25(6)	95.9	93.21(13)	93.14(14)
Cl(2)–Re-E(2)	93.74(7)	92.9	96.69(10)	95.31(12)
Cl(2)–Re–Cl(3)	86.53(7)	86.3	86.5(2)	88.0(2)
E(1)–C(1)–C(2)-E(2)	−0.6(8)	−59.8[a]	−53.4(13)	−53.9(12)[a]
C(1)–C(2)–E(2)–C(31)	109.4(5)	163.7[a]	167.9(10)	171.8(11)[a]
C(1)–C(2)–E(2)–C(41)	−136.9(5)	−81.8[a]	−85.1(11)	−74.7(11)[a]
C(2)–C(1)–E(1)–C(11)	−108.8(5)	−76.4[a]	−86.2(13)	−81.1(13)[a]
C(2)–C(1)–E(1)–C(21)	137.8(5)	173.7[a]	164.8(12)	163.3(11)[a]
Re–E(1)–C(11)–C_{ortho}	72.6(6) [C16]	28.9[a]	64(1) [C12]	68(2) [C56][a]
Re–E(1)–C(21)–C_{ortho}	−66.5(6) [C26]	−74.2[a]	−40(2) [C22]	51(2) [C62][a]
Re–E(2)–C(31)–C_{ortho}	−56.2(5) [C36]	−54.2[a]	−30(2) [C32]	−43(2) [C72][a]
Re–E(2)–C(41)–C_{ortho}	74.6(5) [C46]	58.0[a]	46(1) [C46]	61(2)[C86][a]
Re· · ·E(1)E(2)Cl(1)Cl(2)	0.250(1)	0.226	0.153(2)	0.151(2)

[a] The torsion angles calculated from the coordinates reported in the paper correspond to the enantiomeric molecule. Their sign has been changed to make comparisons easier.

"bond-stretch isomerism", but the situation was straightened out in a classic paper by Yoon, Parkin and Reinghold [12]. The normal Re=O and Re–Cl_{trans} bond lengths in molecules of this type are 1.68 and 2.44 Å, respectively. The apparently long Re=O (1.812 Å) and short Re–Cl bonds (2.355 Å) suggest that a sizable fraction of the molecules adopt the other orientation, but the proportion does not reach 50%, since the distances would become equal. For the other $ReOCl_3$(dpae) molecule, the distances (1.890 and 2.196 Å) indicate that the proportion is closer, but still different from, 50%.

The overall connectivity and structure are definitely established unambiguously by our X-ray study. However, the distances and angles should be used with caution, even those between non-disordered atoms, since disorder probably has a small local effect on the positions of atoms that appear not to be disordered.

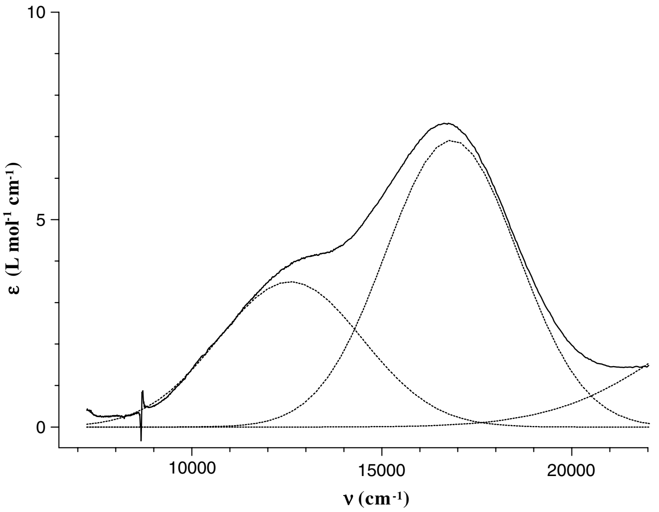

Fig. 4. UV–visible spectra of $ReOCl_3$(dppen) in DMSO (full line). Dashed lines correspond to the two components obtained by deconvolution.

3.3. UV–visible spectroscopy

The typical spectrum of $ReOCl_3$(dppen) is shown in Fig. 4. The ground state (S) and the two lowest-energy singlet states (S* and S**) for this type of systems are schematically represented in Fig. 5. As noted previously for the dppe compounds [2], only two components can be identified in the spectrum, which are assigned to the spin-allowed

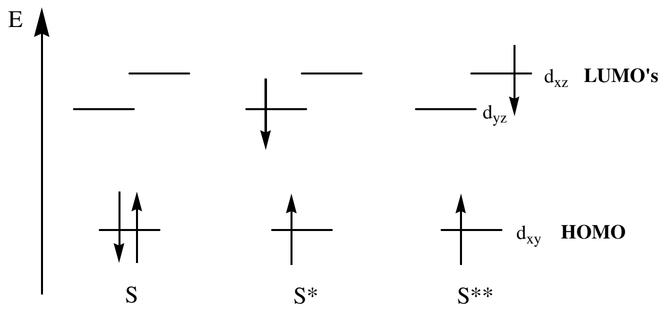

Fig. 5. Low-energy singlet electron configurations for the oxo-Re(V) d^2 systems.

Table 4
Observed transition energies ($cm^{-1} \times 10^3$) [ε] ($L\ mol^{-1}\ cm^{-1}$)

	[S → S*]	[S → S**]
$ReOCl_3(dppe)$[a]	12.0 [13]	16.4 [25]
$ReOCl_3(dppen)$	12.6 [4]	16.8 [7]
$ReOCl_3(dppf)$	12.2 [15]	16.5 [52]
$ReOCl_3(dpae)$	11.3 [22]	16.0 [41]
$ReOCl_2(OEt)(dppe)$[a]	16.4 [12]	20.0 [21]
$ReOCl_2(OEt)(dppen)$	18.4 [18]	19.3 [52]
$ReOCl_2(OEt)(dppf)$	N/O[b]	N/O[b]

[a] In DMSO, Ref. [2].

[b] Masked by a strong absorption of the dppf ligand.

transitions of an electron to the two LUMO orbitals, respectively. These bands may be used to make comparisons with the dppe systems. The data are given in Table 4. $ReOCl_2(OEt)(dppf)$ cannot be included, since the d–d transitions are masked by the strong ligand band at 22700 cm^{-1}, located in the ferrocene moiety. The trend noted earlier for an alkoxo group to increase the transition energy is obeyed here, the first transition of dppen moving from 12600 to 18400 cm^{-1}.

With respect to $ReOCl_3(dppe)$, substitution by another diphosphine induces a small displacement to higher energy, but the change is not spectacular. On the other hand, introducing the arsine donor groups of dpae produces a modest decrease of the transition energies by 700 cm^{-1} for S → S* and 400 cm^{-1} for S → S**. Thus, at the moment, the $ReOCl_3(dpae)$ complex is the mono-oxorhenium(V) compound with the smallest HOMO–LUMO energy gap, slightly below those of the $ReOCl(P{\sim}O)_2$ complexes (11900 and 16000 cm^{-1}) [1].

The gap between the two singlet states of the trichloro compounds is ~4000 cm^{-1}, similar to those observed by Baril-Robert [2] for the trichloro and tribromo $ReOX_3$(dppe) compounds. However, for the $ReOX_2(OR)(dppe)$ compounds, a gap of ~3000 cm^{-1} was found, whereas a smaller value of ~900 cm^{-1} is observed here with $ReOCl_2(OEt)(dppen)$.

4. Concluding remarks

The $ReOCl_3(L–L)$ and $ReOCl_2(OEt)(L–L)$ compounds studied here obey the normal trends in oxo-rhenium(V) compounds, since they adopt the *fac*-trichloro and *trans*-oxo-ethoxo arrangements, respectively. The visible spectra of the dppen and dpae compounds are similar to those of related dppe compounds. Replacing the central $–CH_2–CH_2–$ section by a more rigid $–C(H){=}C(H)–$ unit does not produce drastic changes on the HOMO–LUMO gap. Although the replacement of P by softer As donors produces a small shift to the transition to lower energies, this change is rather modest.

Acknowledgements

We wish to thank Dr. M. Simard and F. Bélanger-Gariépy for assistance in the interpretation of the X-ray diffraction data, and the Natural Sciences and Engineering Research Council of Canada for financial support.

Appendix A. Supporting information

Crystallographic data for $ReOCl_3(dpae)$ and $ReOCl_3$(dppen) have been deposited with the Cambridge Crystallographic Data Center, CCDC nos. 267886 and 267887, respectively. Copies of these information may be obtained free of charge on application to CCDC, 12 Union Road, Cambridge CB2 1EZ, UK (fax: +44 1223 336033; e-mail: deposit@ccdc.cam.ac.uk or http://www.cam.ac.uk).

References

[1] U. Oetliker, C. Savoie, S. Stanislas, C. Reber, F. Connac, A.L. Beauchamp, F. Loiseau, M. Dartiguenave, J. Chem. Soc., Chem. Commun. (1998) 657.
[2] F. Baril-Robert, A.L. Beauchamp, Can. J. Chem. 81 (2003) 1326.
[3] J. Chatt, G.A. Rowe, J. Chem. Soc. (1962) 4019.
[4] D.E. Grove, G. Wilkinson, J. Chem. Soc. A (1966) 1224.
[5] J.C. Bryan, R.E. Stenkamp, T.H. Tulip, J.M. Mayer, Inorg. Chem. 26 (1987) 2283.
[6] C. Imrie, J.R. Dilworth, Y. Zheng, A.R. Abrahams, T.I.A. Gerber, V.O. Nyamori, J. Chem. Soc. Dalton Trans. (2001) 2624.
[7] X.L. Luo, R.H. Crabtree, J. Am. Chem. Soc. 112 (1990) 4813.
[8] CAD-4 Software, version 5.0. Enraf-Nonius, Delft, The Netherlands, 1989.
[9] G.M. Sheldrick, SHELXTL, The Complete Software Package for Single Crystal Structure Determination, Release 5.10., Bruker AXS Inc., Madison, WI, USA, 1997.
[10] SMART, Bruker Molecular Analysis Research Tool, Release 5.059. Bruker AXS Inc., Madison, WI, USA, 1999.
[11] SAINT, Integration Software for Single Crystal Data, Release 6.06. Bruker AXS Inc., Madison, WI, USA, 1999.
[12] K. Yoon, G. Parkin, A.L. Rheingold, J. Am. Chem. Soc. 114 (1992) 2210.
[13] A.M. Lebuis, A.L. Beauchamp, Can. J. Chem. 71 (1993) 441.
[14] A.L. Spek, PLATON, Molecular Geometry Program, University of Utrecht (Holland), Utrecht, 2000.
[15] O. Knoesen, H. Görls, S. Lotz, J. Organometal. Chem. 598 (2000) 108.
[16] B. Jezowska-Trzebiatowska, J. Hanuza, M. Baluka, Spectrochim. Acta A 27 (1971) 1753.
[17] O. Sigouin, A.L. Beauchamp, Acta Crystallogr., Sect. E61 (2005) m736.
[18] J.P. O'Neil, S.R. Wilson, J.A. Katzenellenbogen, Inorg. Chem. 33 (1994) 319.

[19] M.S. Papadopoulos, M. Pelecanou, I.C. Pirmettis, D.M. Spyriounis, C.P. Raptopoulou, A. Terzis, C.I. Stassinopoulou, E. Chioellis, Inorg. Chem. 35 (1996) 4478.
[20] J.C.C. Gómez, F.J.S. López, MestRe-C, 2004.
[21] V.S. Sergienko, M.A. Porai-Koshits, V.E. Mistryukov, K.V. Kotegov, Koord. Khim. 8 (1982) 230.